

Supporting Information

for

New Water-Soluble Oxyamino Chitosans as
Biocompatible Vectors for Efficacious
Anticancer Therapy via Co-Delivery of
Gene and Drug

*Mohini Kamra,^{†,§} Parikshit Moitra,[†] Devasena Ponnalagu,^{‡,⊥} Anjali A. Karande,[‡] and Santanu
Bhattacharya^{†,§,||,*}*

[†]Technical Research Centre and ^{||}School of Applied and Interdisciplinary Sciences, Indian Association for the Cultivation of Science, Kolkata 700032, West Bengal, India.

[§]Department of Organic Chemistry and [‡]Department of Biochemistry, Indian Institute of Science, Bangalore 560012, Karnataka, India.

*Email address of the corresponding author: sb23in@yahoo.com, director@iacs.res.in,
sb@iisc.ac.in

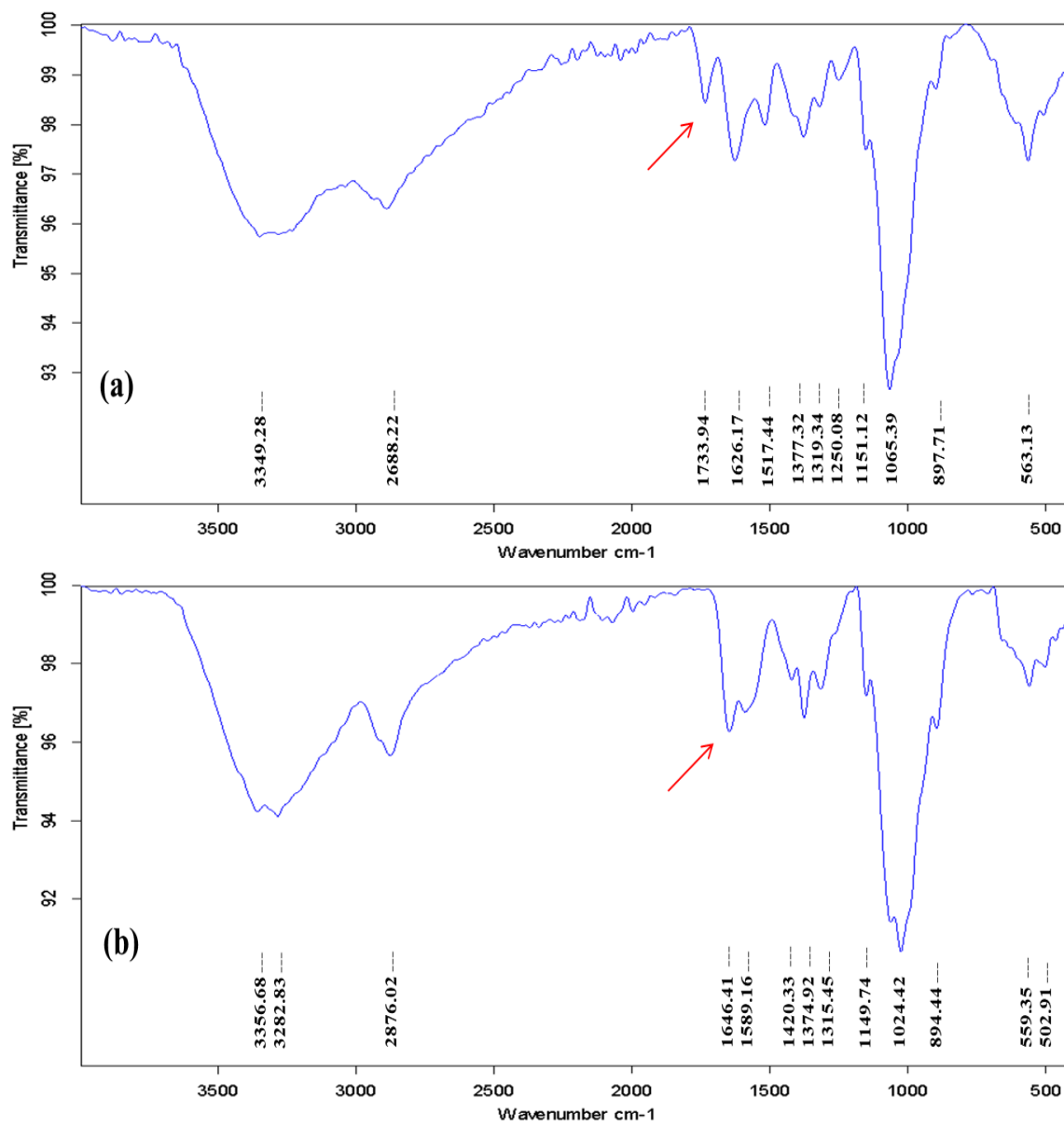


Figure S1. FT-IR spectra of (a) CS(CH₂COOH) and (b) CS taken as KBr pellet.

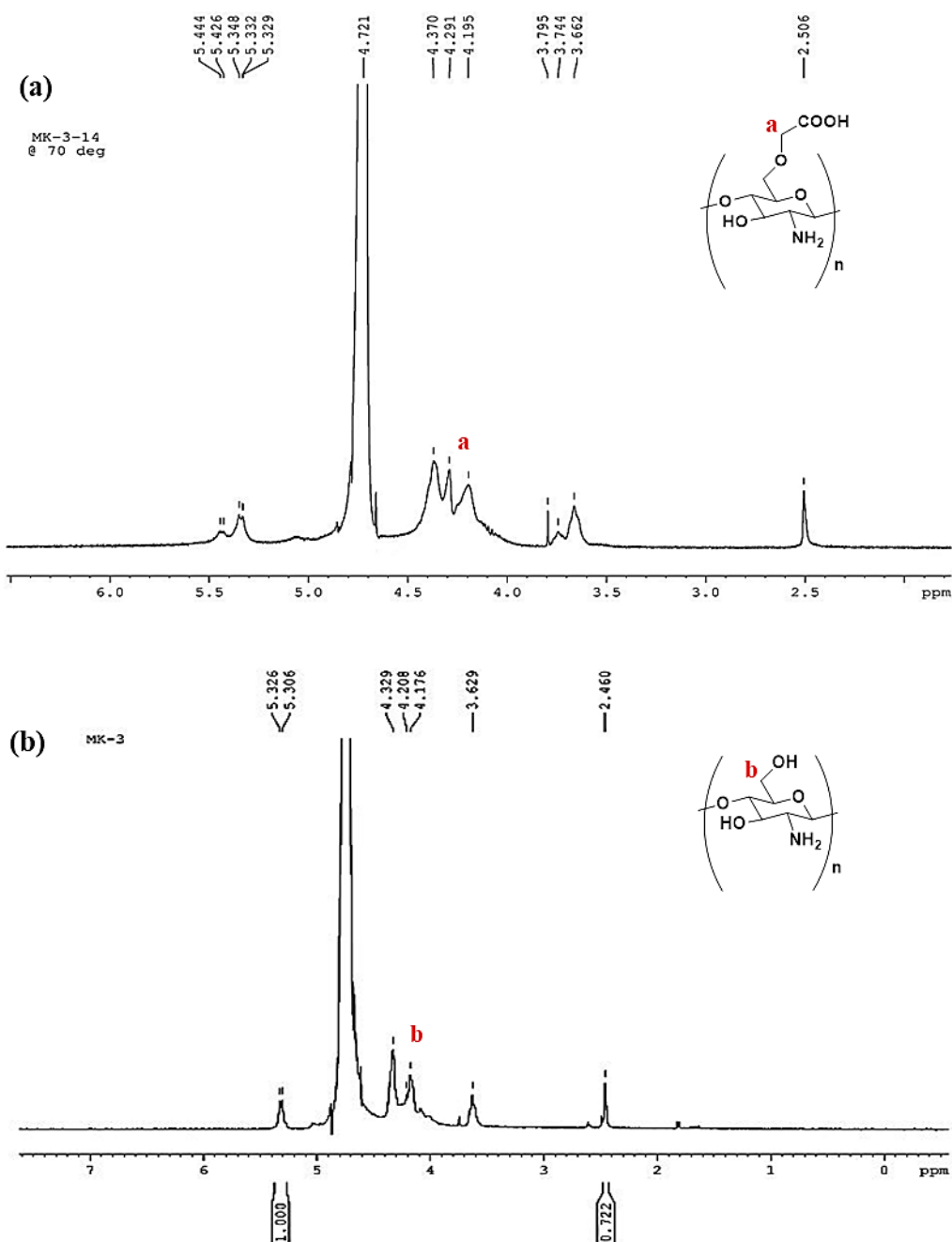


Figure S2. $^1\text{H-NMR}$ spectra of (a) $\text{CS}(\text{CH}_2\text{COOH})$ and (b) CS in D_2O and $\text{HCl}/\text{D}_2\text{O}$ respectively.

Table S1. Synthesized CS(CH₂COOH) of Different Degrees of Substitution.

Equiv. of ClCH₂COOH used	%Degree of carboxymethylation	Water solubility
2	8	Insoluble in water
4	25	Soluble in water
8	60	Soluble in water

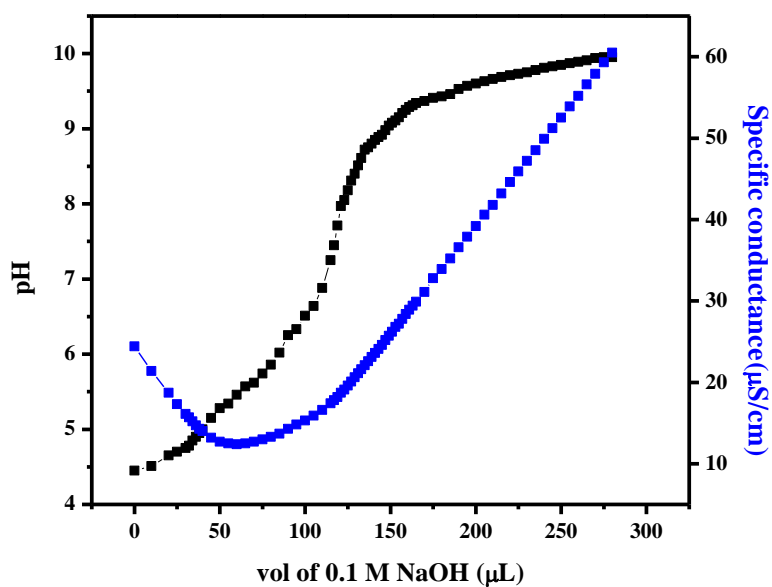


Figure S3. Conductometric and pHmetric titration curves for CS(CH₂COOH) with 25% degree of carboxymethylation.

Table S2. Synthesized (py)CS(CH₂COOH) of Different Degrees of Substitution.

Equiv. of pyridine aldehyde used	%Degree of pyridine substitution	Water solubility
2	8	Soluble in water
4	47	Soluble in water
8	47	Soluble in water

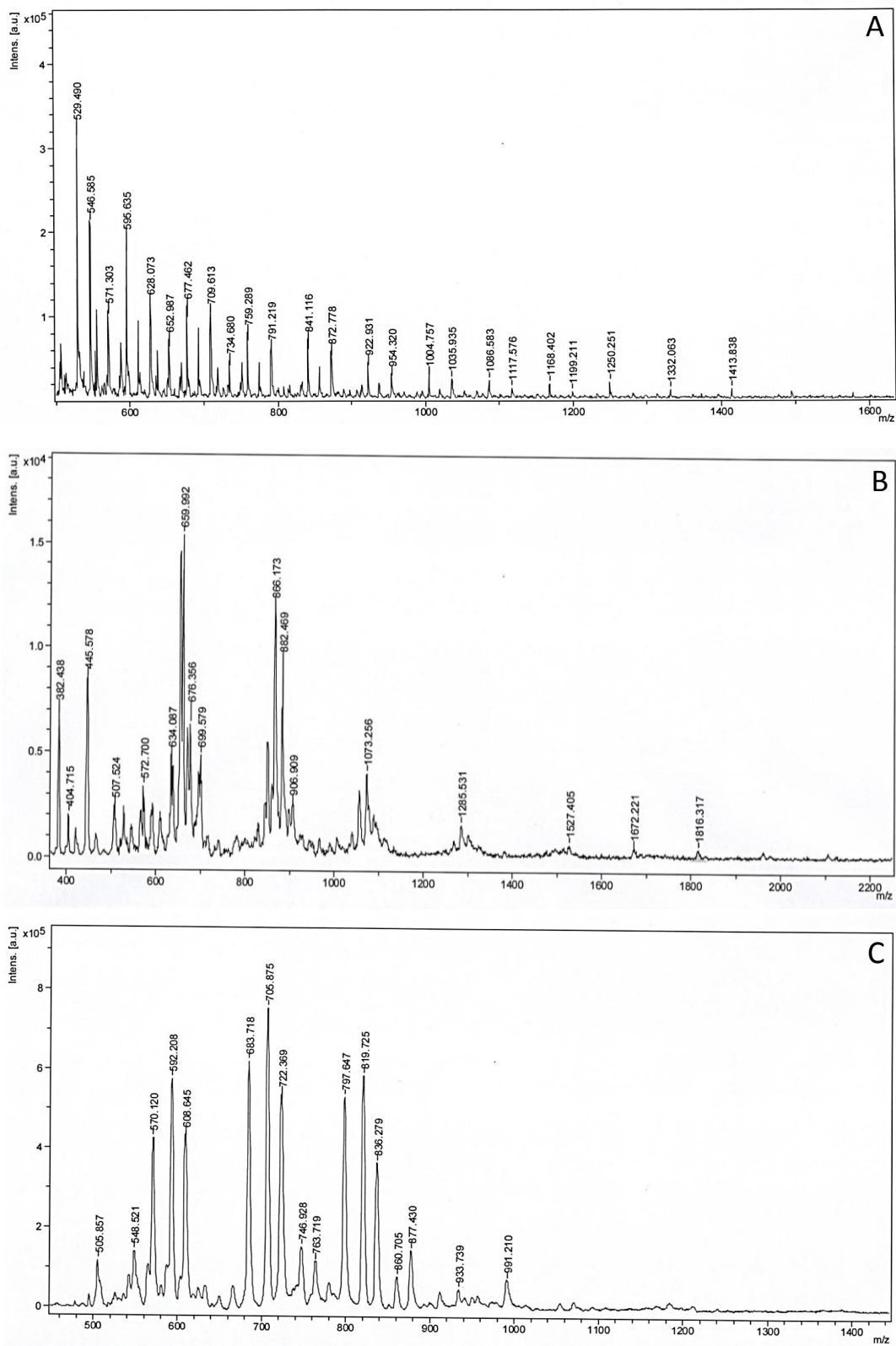


Figure S4. MALDI-TOF MS of (A) CS (B) CS(CH₂COOH) and (C) (py)CS(CH₂COOH) using α -Cyano-4-hydroxycinnamic acid (CHCA) matrix in 1:1 ratio.

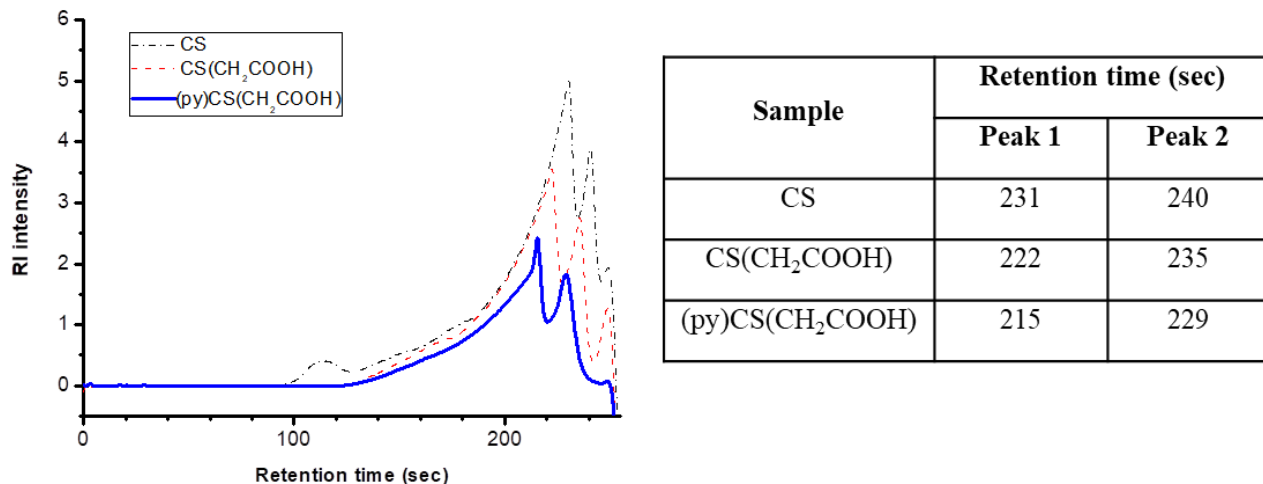


Figure S5. GPC traces of CS, CS(CH₂COOH) and (py)CS(CH₂COOH) recorded in isocratic mode at 40 °C, 0.5 mL/min flow rate in water. Retention times are shown on the right.

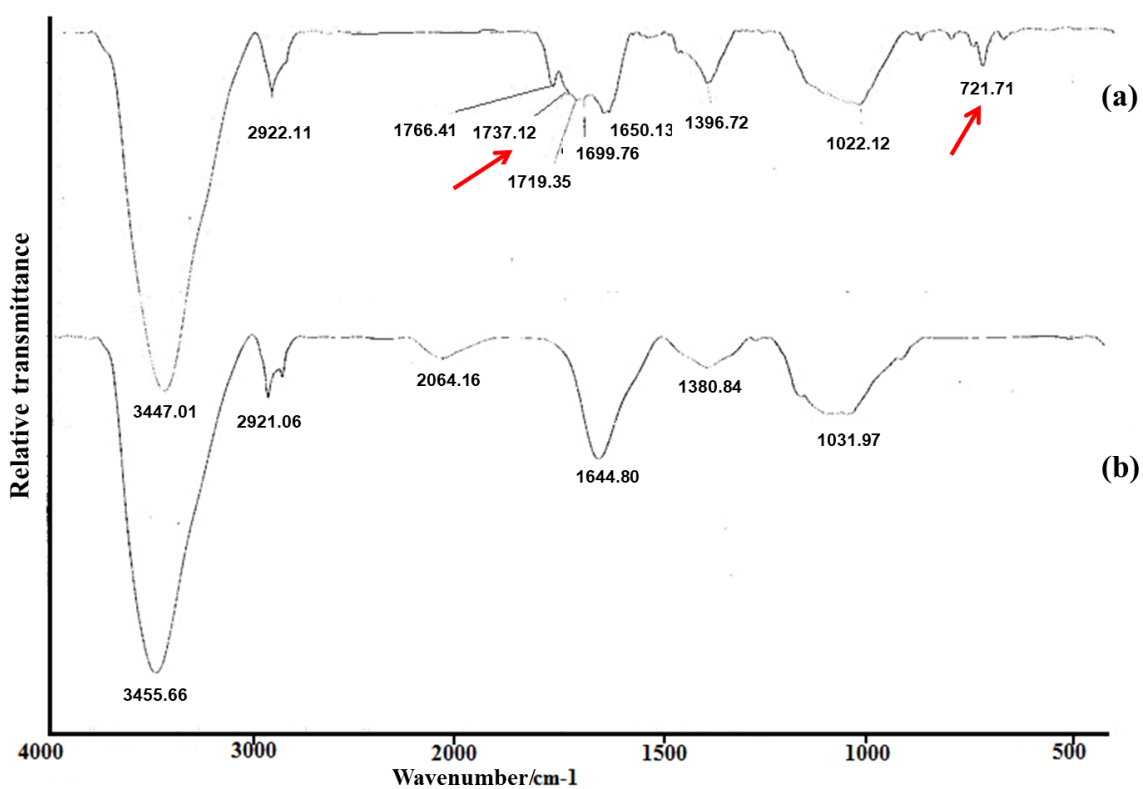


Figure S6. FT-IR spectra of (a) *N*-phthaloyl chitosan and (b) chitosan, taken as KBr pellet, depicting the introduction of phthaloyl protecting group.

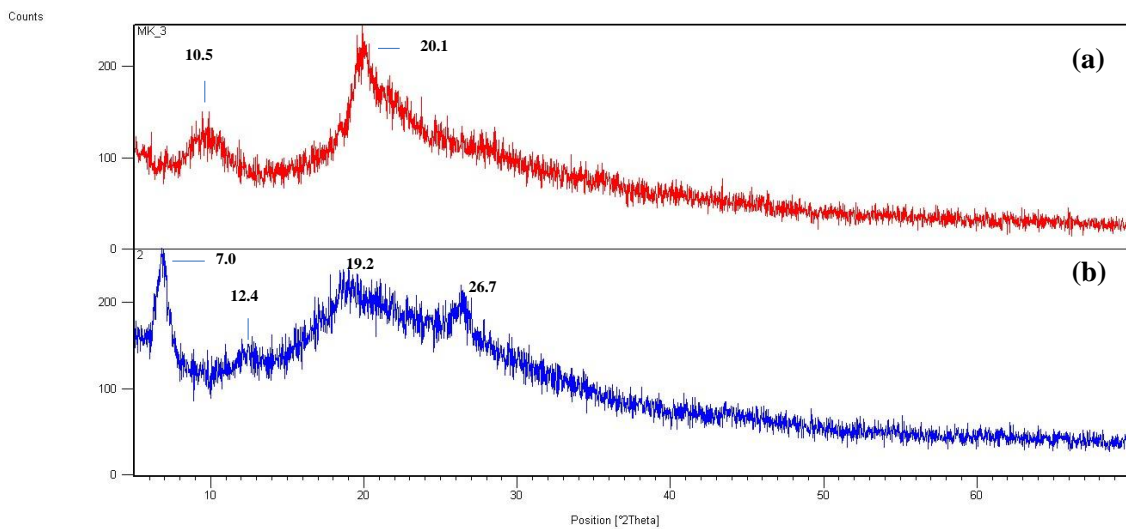


Figure S7. X-ray diffraction patterns of (a) chitosan and (b) phthaloyl chitosan depicting no loss in crystallinity and maintenance of organized structures.

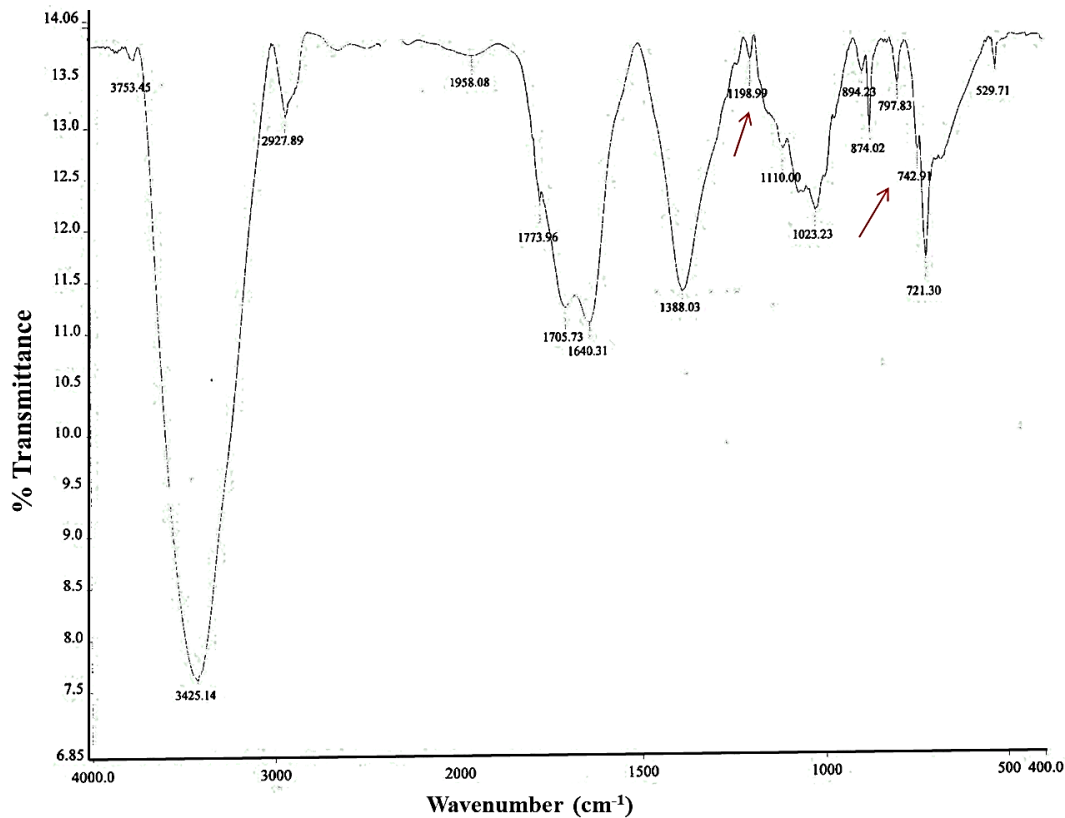


Figure S8. FT-IR spectrum of 6-O-tosyl-N-phthaloyl chitosan, taken as KBr pellet, depicting the incorporation of tosyl group after phthaloyl protection of primary amines.

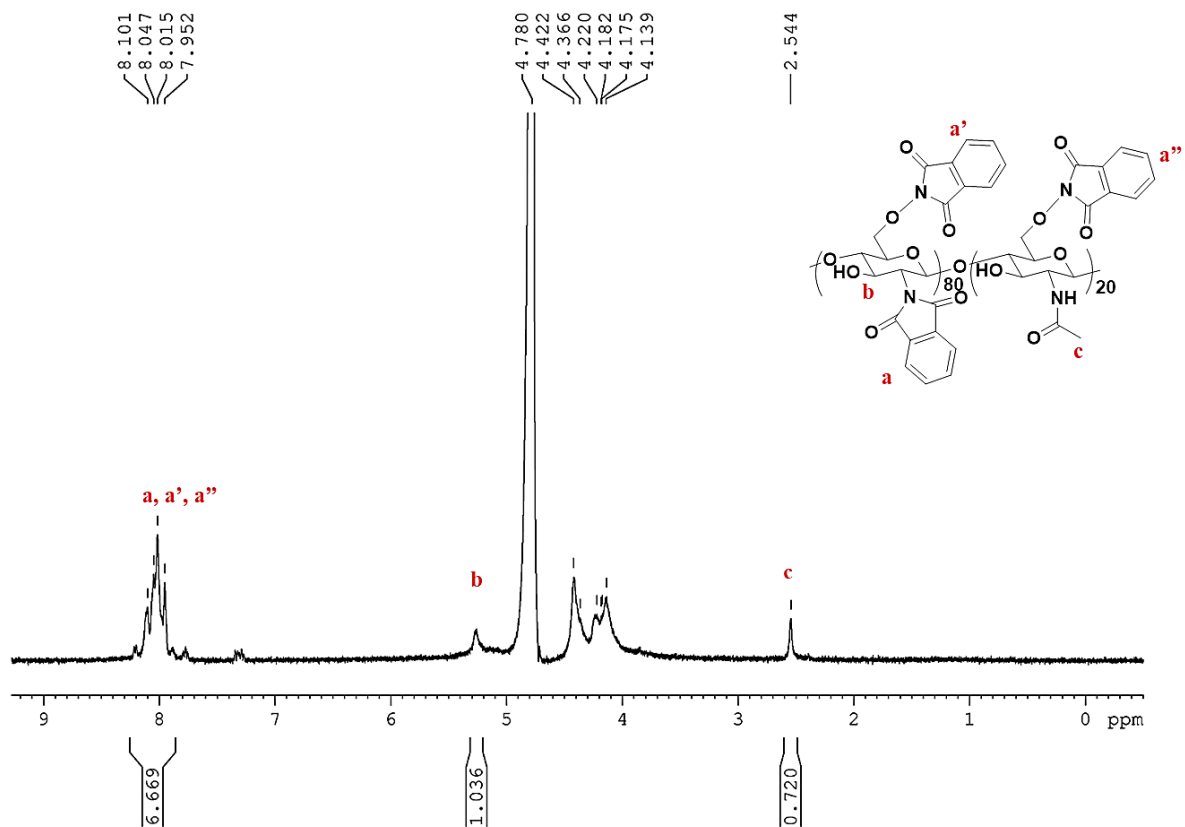


Figure S9. $^1\text{H-NMR}$ spectrum of di-phthaloyl substituted chitosan indicating about 40% degree of substitution.

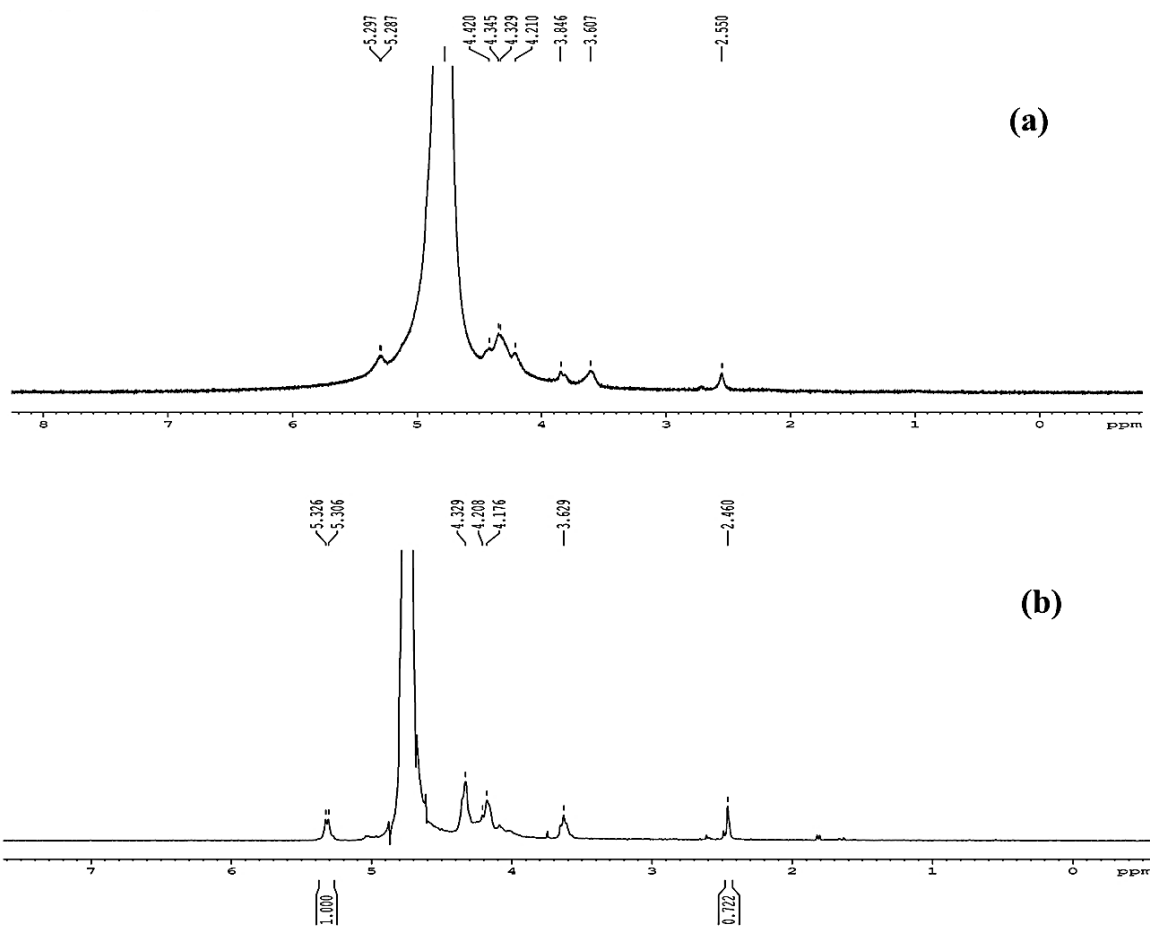


Figure S10. Comparison of $^1\text{H-NMR}$ of (a) CS(OH₂) and (b) CS in D₂O solvent at 70 °C.

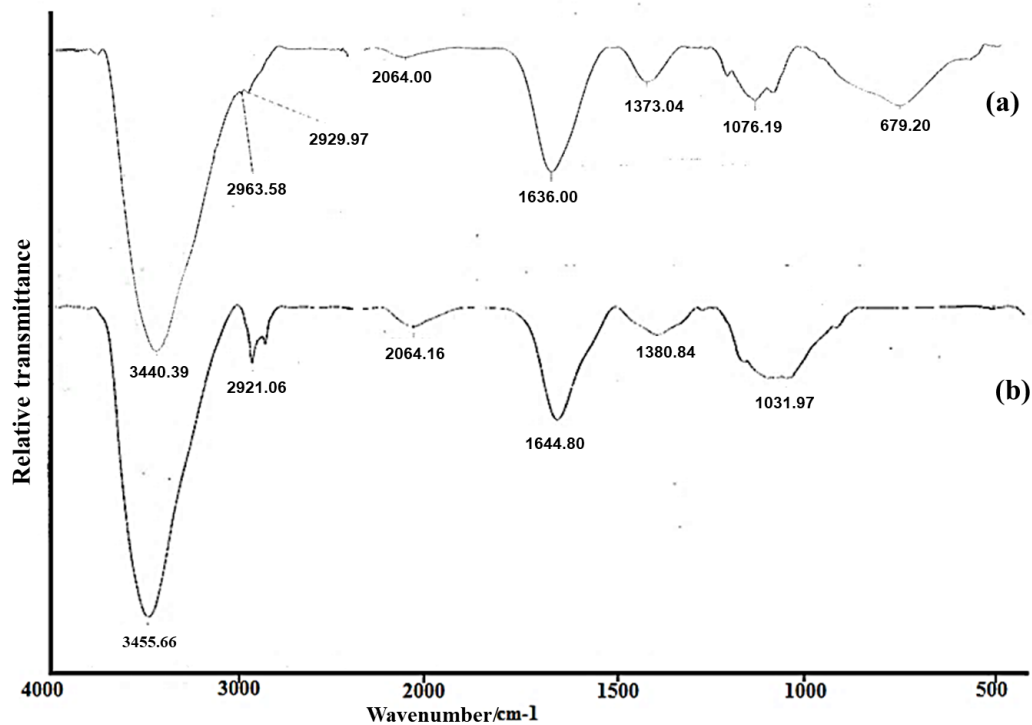


Figure S11. Comparison of FT-IR spectra of (a) CS(OH₂) and (b) CS, taken as KBr pellet.

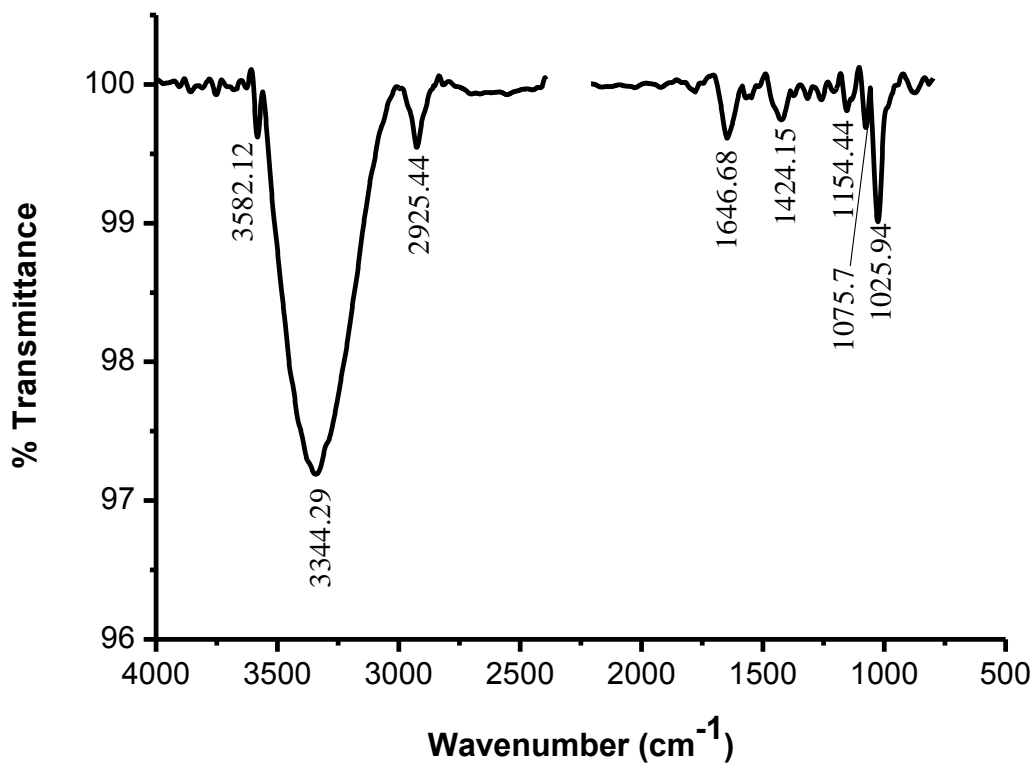


Figure S12. FT-IR spectrum of CS(Dox) oxime ether indicating the functional groups present.

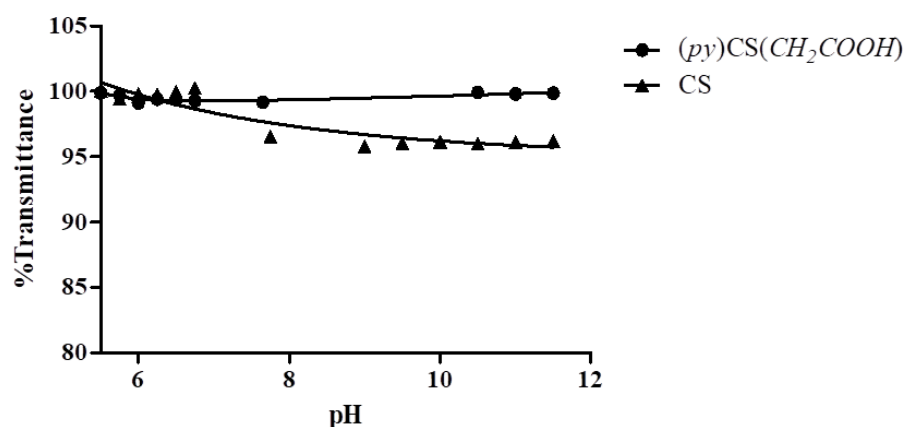


Figure S13. Cloud point estimation of the native and functionalized chitosan using UV-Vis Spectroscopy. % Transmittance at 600 nm, measured in a 1cm quartz cell, was plotted against pH of the solution.

Table S3. Average Hydrodynamic Diameter Changes with Time in PBS^a

Days (in PBS)	1	2	3	4	5	6	7
(py)CS(CH ₂ COOH)/ pEGFP-C3	95 ± 5	97 ± 3	98 ± 5	100 ± 3	101 ± 4	105 ± 5	104 ± 7
CS(Dox)	200 ± 10	202 ± 5	202 ± 7	205 ± 5	210 ± 4	207 ± 7	210 ± 6

^aFormulations were prepared in PBS, pH 7.4 and maintained at 25 °C for the designated time duration.

Table S4. Average Hydrodynamic Diameter Changes with Time in RPMI 1640^b

Days (in RPMI)	1	2	3	4	5	6	7
(py)CS(CH ₂ COOH)/ pEGFP-C3	100 ± 4	105 ± 5	105 ± 8	107 ± 4	108 ± 4	110 ± 5	114 ± 4
CS(Dox)	210 ± 3	212 ± 5	212 ± 6	215 ± 7	217 ± 6	219 ± 5	221 ± 5

^bFormulations were prepared in RPMI 1640 and maintained at 25 °C for the designated time duration

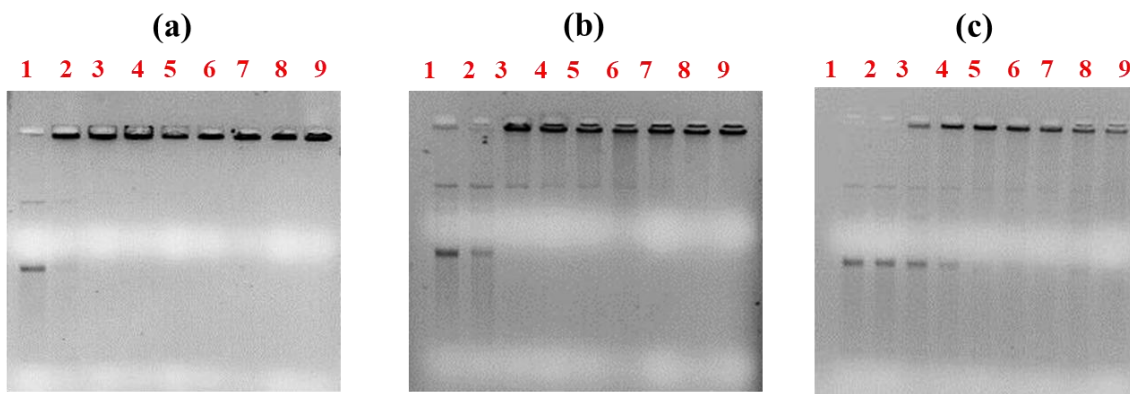


Figure S14. DNA Mobility Shift Assay for determination of degree of binding of (a) CS, (b) CS(CH₂COOH) and (c) (py)CS(CH₂COOH) to pDNA. Lane 1: DNA alone, Lane 2-9: N/P = 1,2,5,10,20,50,80,100 respectively. ([pEGFP] = 0.5 μg/well).

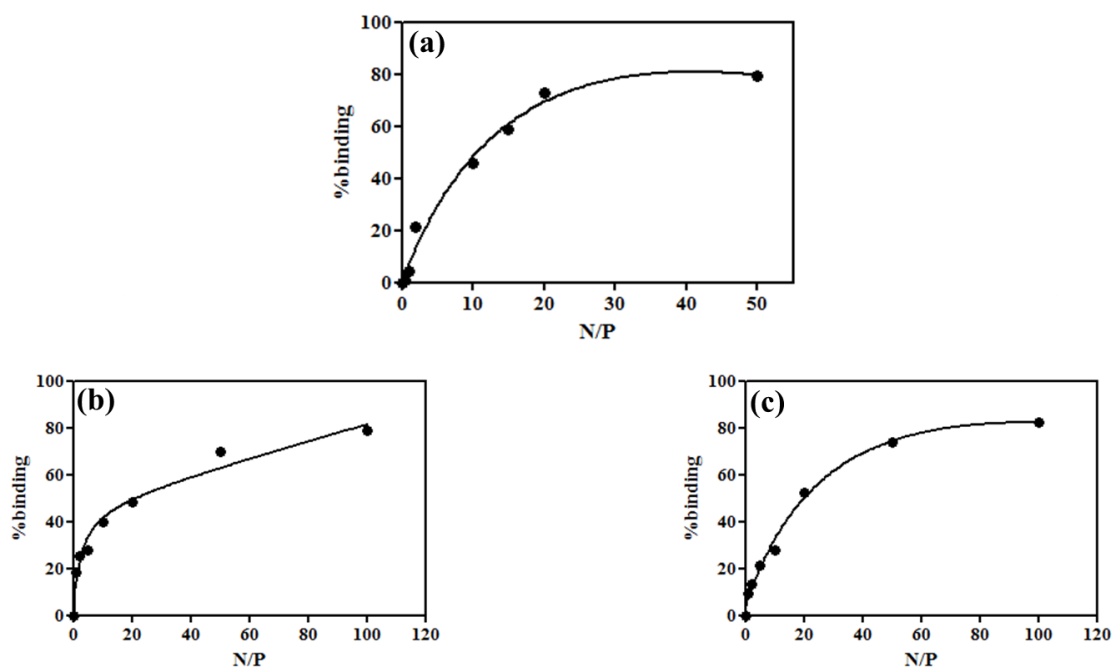


Figure S15. Polymer/DNA binding curves for (a) CS, (b) CS(CH₂COOH) and (c) (py)CS(CH₂COOH) based on Ethidium bromide fluorescence assay.

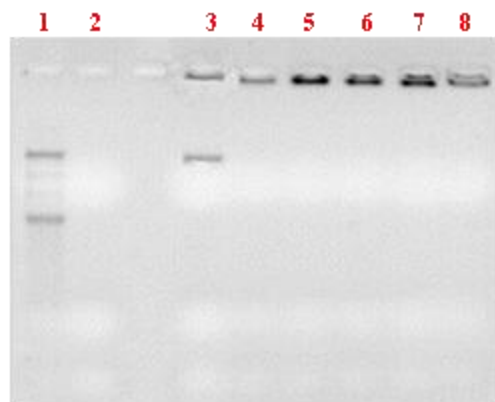


Figure S16. Protection of pDNA in (py)CS(CH₂COOH) polyplex against DNase I digestion. Lane 1 : DNA alone; Lane 2: Naked DNA + DNase; Lane 3, 5, 7 :Polymer/DNA complex at N/P = 5, 20, 40 respectively; Lane 4, 6, 8 :Polymer/DNA complex at N/P = 5, 20, 40 respectively, each mixed with DNase ([pEGFP] = 0.5 μg/well).

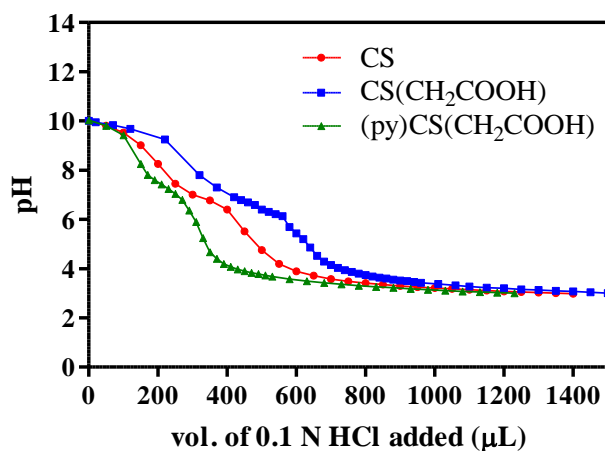


Figure S17. Assessment of polymer buffering capacity at room temperature. Plot of pH vs. volume of acid added to CS, CS(CH₂COOH) and (py)CS(CH₂COOH) in aqueous solution.

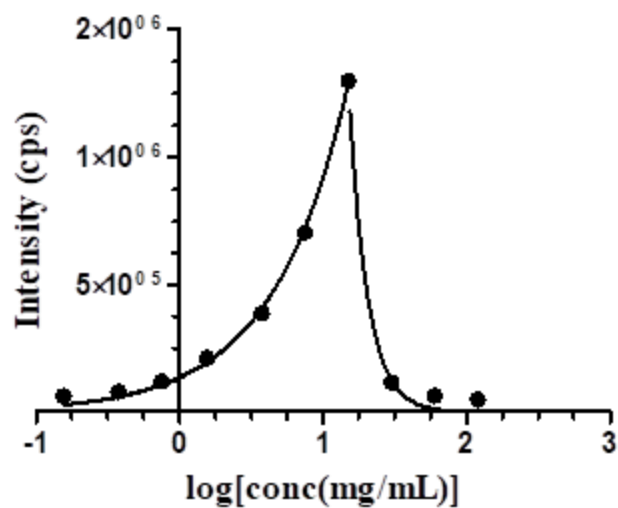


Figure S18. Fluorescence intensity of Doxorubicin (Dox) as a function of polymer concentration in the nano-composite CS(Dox) + (py)CS(CH₂COOH)/pDNA.

Table S5. IC₅₀ of Various Formulations in HEK 293T cell line.^c

Formulation	(py)CS(CH ₂ COOH)/p53	Dox alone	(py)CS(CH ₂ COOH)/p53 + Dox	CS(Dox)	(py)CS(CH ₂ COOH)/p53 + CS(Dox)
IC ₅₀ (μg/mL)	> 15	3.9± 0.5	1.4 ± 0.1	1.95 ± 0.1	1.26 ± 0.03

^cFormulations were prepared in culture medium and incubated with the cells at 37 °C for 48 h.

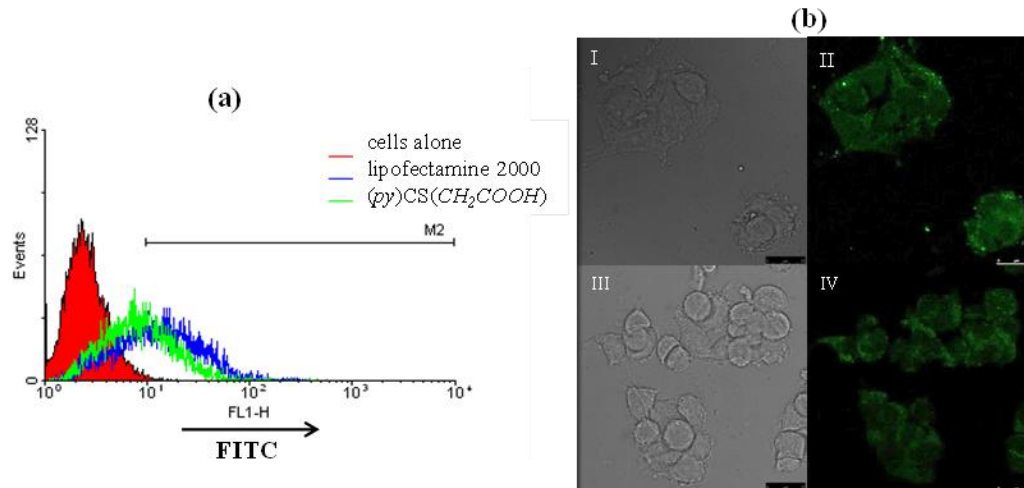


Figure S19. Internalization of Fluorescein labelled pGL3-control plasmid. HEK 293T cells were treated with the polyplex/lipoplex containing the labelled plasmid for 4 h. (a) FACS analysis shows the histogram for the FL1 channel. (b) Confocal Microscopy shows the bright field images (I and III) as well as fluorescence images (II and IV) using a 488 nm excitation laser. (py)CS(CH₂COOH) (III and IV) and Lipofectamine 2000 (I and II). Scale bar = 25 μm.

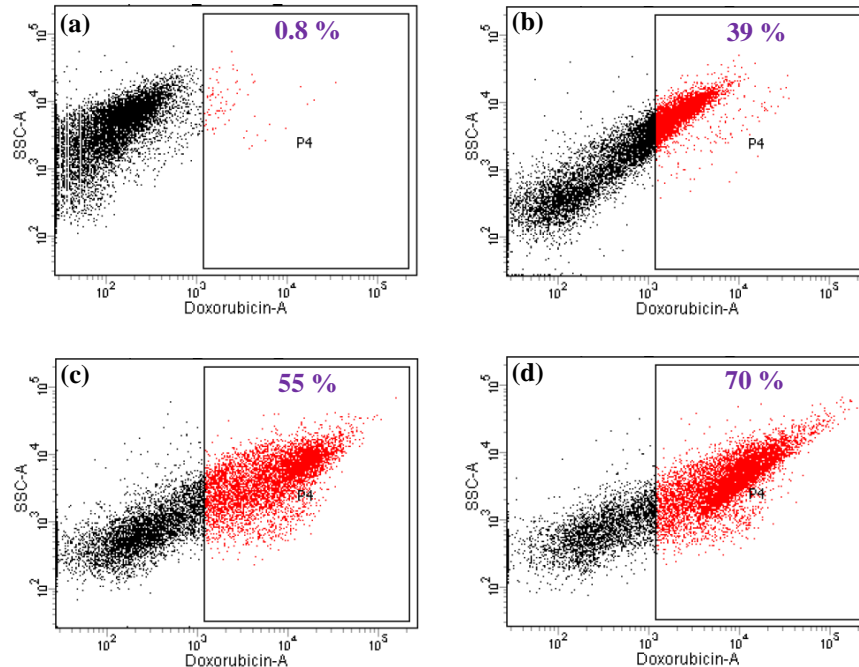


Figure S20. Assessment of Doxorubicin uptake of HEK 293T cells in presence of (b) free drug, (c) CS(Dox) and (d) composite of CS(Dox) with (py)CS(CH₂COOH) in the culture medium. Panel (a) represents untreated cells control.

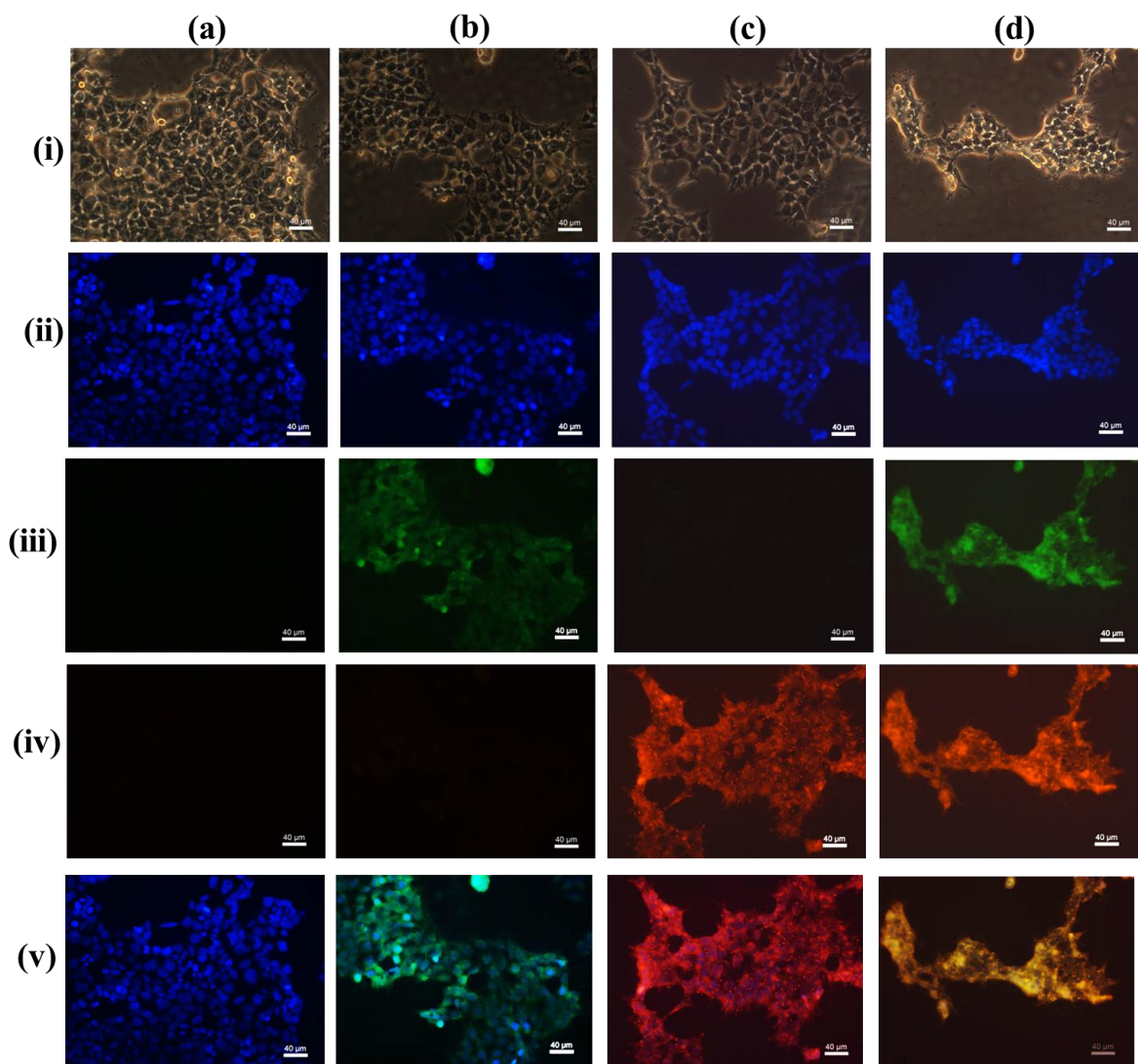


Figure S21. Representative fluorescence microscopy images for (a) cells alone, (b) (py)CS(CH₂COOH)/Fluor-pGL3, (c) CS(Dox) and (d) composite of CS(Dox) and (py)CS(CH₂COOH)/Fluor-pGL3, 4 h after respective treatments. Panels (i), (ii), (iii) and (iv) represent BF, DAPI, FITC and Dox channels, respectively; Panel (v) represents the overlay of images. Scale bar = 40 μm.

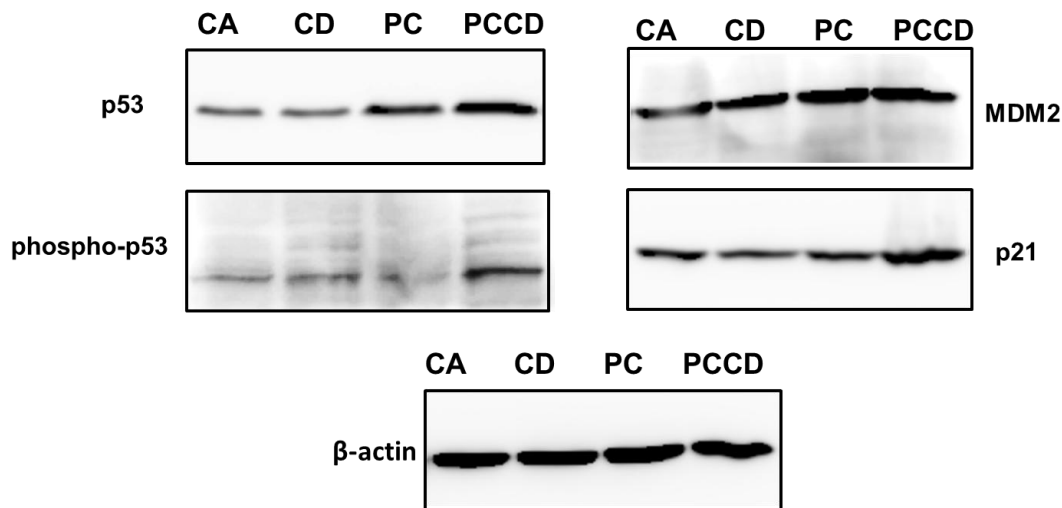


Figure S22. Western blot analysis for the assessment of p53 phosphorylation products and p53 target genes upon treatment of HEK 293T cells with the respective formulations. [CA: Cells alone; CD: CS(Dox); PC: p53/(py)CS(CH₂COOH); PCCD: p53/(py)CS(CH₂COOH) + CS(Dox)]

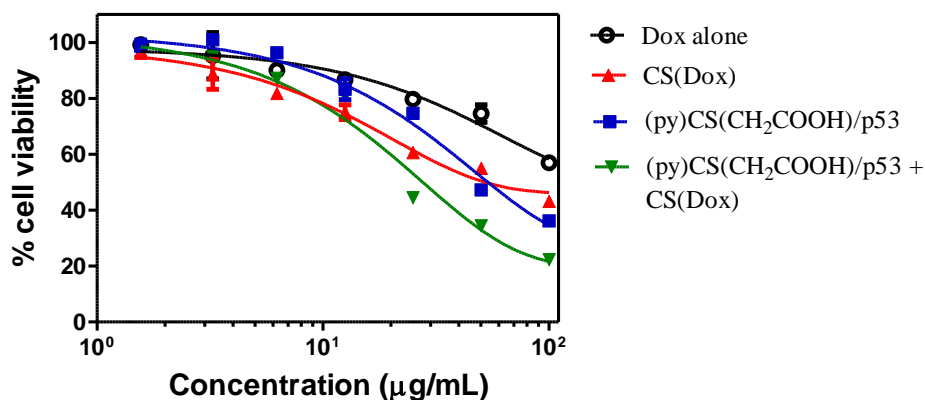


Figure S23. MTT Assay for determination of cytotoxicity of CS(Dox) and its composite polyplexes (at 1:1 molar ratio) with (py)CS(CH₂COOH)/p53 carrying pCEP4-p53 in CT26 cell line. Comparison with Dox alone is also shown.

Table S6. IC₅₀ of Various Formulations in CT26 cell line.^d

Formulation	IC ₅₀ (µg/mL)
Dox alone	> 100
CS(Dox)	51 ± 5
(py)CS(CH ₂ COOH)/p53	56 ± 6
(py)CS(CH ₂ COOH)/p53 + CS(Dox)	30 ± 3

^dMTT assay was performed after treatment for 48 h at 37 °C.

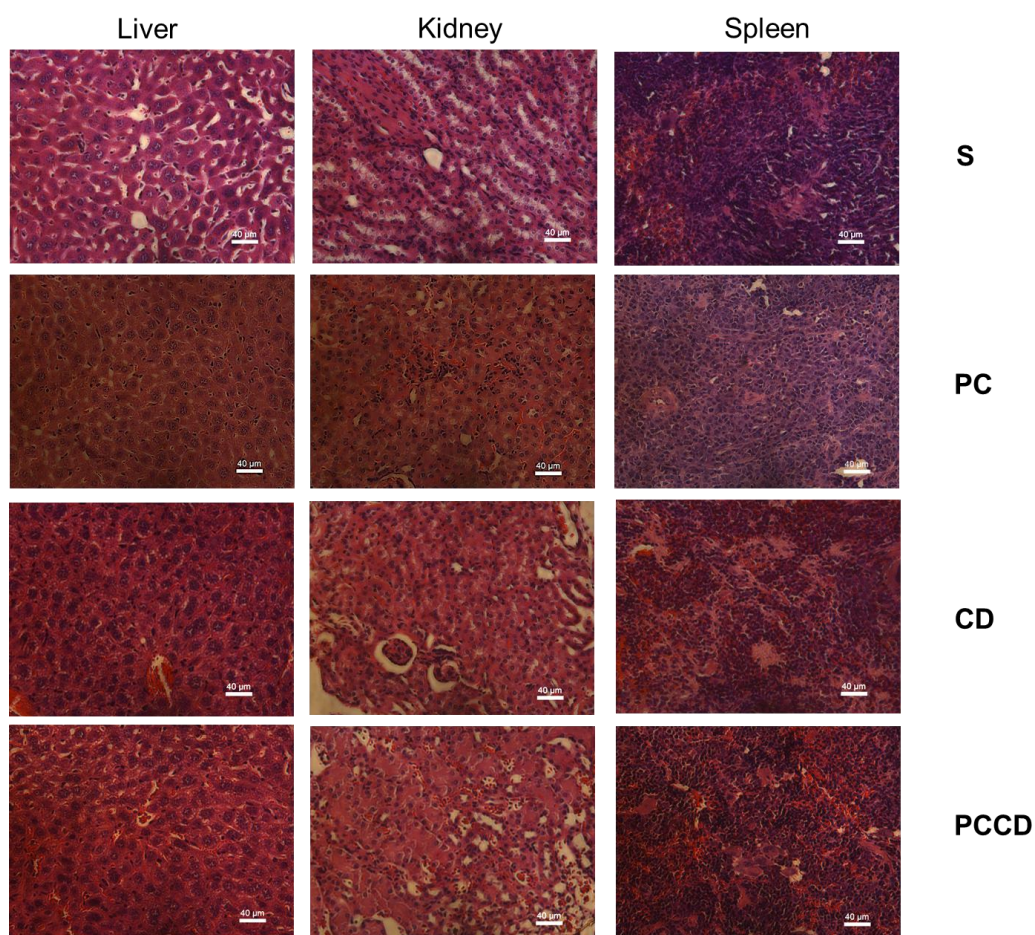


Figure S24. Representative images for histology analysis of effect of various treatments. Vital organs of Balb/c mice were excised and sections were stained using haematoxylin and eosin followed by imaging under 40X objective. [S: Saline control; CD: CS(Dox); PC: (py)CS(CH₂COOH)/p53 polyplex; PCCD: CS(Dox) + (py)CS(CH₂COOH)/p53 polyplex]. Scale bar = 40 µm.

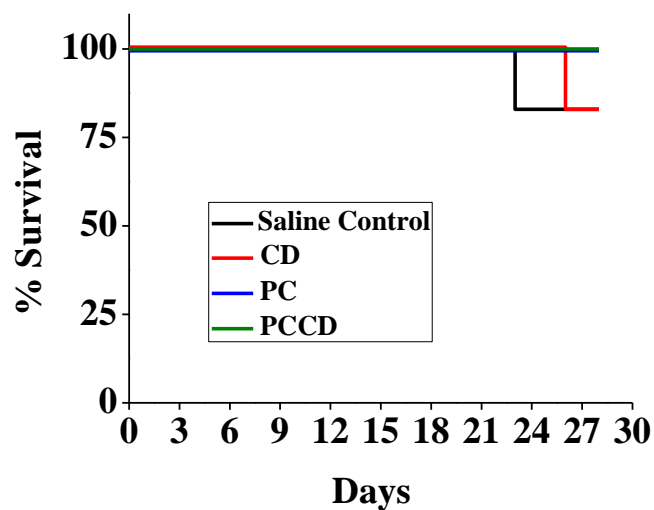


Figure S25. Survival plot for Balb/c mice injected with different formulations: CD: CS(Dox); PC: (py)CS(CH₂COOH)/p53 polyplex; PCCD: CS(Dox) + (py)CS(CH₂COOH)/p53 polyplex.

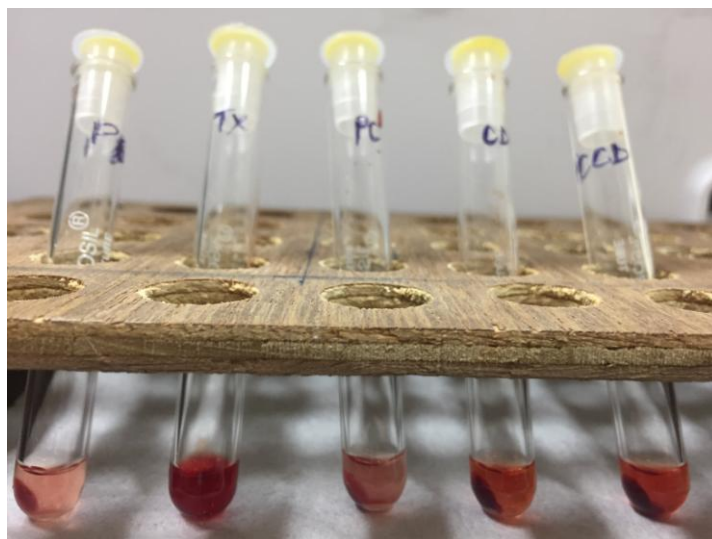


Figure S26. Photograph of hemolysis studies. Degree of hemolysis, against Triton X-100, in presence of various formulations incubated for 1 h at 37 °C with mouse RBC's. [CD: CS(Dox); PC: (py)CS(CH₂COOH)/p53 polyplex; PCCD: CS(Dox) + (py)CS (CH₂COOH)/p53 polyplex]

Table S7. Hemocompatibility Assessment of Designed Formulations^e

Sample	Clotting time (min)	% hemolysis
PBS	2.5 ± 0.2	0.0
Positive Control	1.0 ± 0.1	100
PC	2.4 ± 0.2	2.6 ± 0.3
CD	2.2 ± 0.1	3.9 ± 0.3
PCCD	2.5 ± 0.2	4.9 ± 0.4

^eFormulations were diluted in PBS and incubated with RBC's isolated from mouse blood. [CD: CS(Dox); PC: (py)CS(CH₂COOH)/p53 polyplex; PCCD: CS(Dox) + (py)CS(CH₂COOH)/p53 polyplex, Positive control = PEI (for clotting time) and Triton X-100 (for hemolysis)]

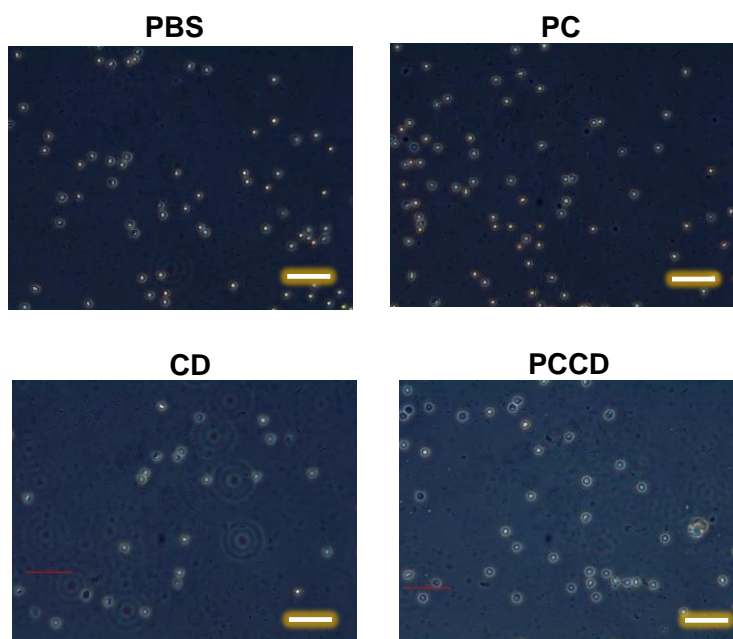


Figure S27. Hemoagglutination assay. Phase contrast micrographs of mouse RBC's incubated with the various formulations at 37 °C for 30 min. Scale bar = 40 μm. [CD: CS(Dox); PC: (py)CS(CH₂COOH)/p53 polyplex; PCCD: CS(Dox) + (py)CS (CH₂COOH)/p53 polyplex]

EXPERIMENTAL DETAILS OF THE BIOPHYSICAL STUDIES

Determination of degree of carboxymethylation. pHmetric and conductometric titrations were carried out using pH meter (ThermoScientific) and conductometer (Control Dynamics, APX 185) in order to determine the degree of *O*-carboxymethylation. 5 mg of the CS(CH₂COOH) was dissolved in 50 mL of water. To this aliquots of freshly prepared 0.1 M NaOH solution were added while monitoring pH and conductance. For the water insoluble derivative, 0.1 M HCl was first added to dissolve the compound, then titrated against 0.1 M NaOH.

Determination of polymer solubility. The water solubility of the parent and derivatized chitosan was estimated using the method of Park *et al*¹ with minor modifications from Anderson *et al*.² 0.2 mg/mL solutions of CS and (py)CS(CH₂COOH) were prepared in 0.1M Sodium Acetate buffer pH 5.5. These were gradually titrated using small volumes of a 1M NaOH solution and % Transmittance (%T) spectra were recorded at various pH using Shimadzu UV-2100 spectrophotometer, in a quartz cell with an optical path length of 1cm. The values of %T at 600nm were plotted against pH using GraphPad Prism 5 software. The plot was then used to compute the cloud point pH values, i.e. the pH upto which, the % transmittance did not fall below 98%.³

Preparation of polyplex formulations. Amount of CS, CS(CH₂COOH) and (py)CS(CH₂COOH) to be taken for complexation was calculated from charge ratios taking 330 Da as the average molar mass per unit charge for DNA. Equal volumes of dilutions in 0.1 M sodium acetate buffer of pH 5.5 were prepared for both pDNA and (py)CS(CH₂COOH) (from a 2 mg/mL stock solution that has been freshly sonicated for 15 minutes at room temperature).

These were heated for 5 minutes at 55 °C, mixed and immediately vortexed for 30 seconds. The mixture was incubated at room temperature for another half an hour for polyplex formation. These polyplexes were diluted in cell culture medium or deionised water as required for further study. Composites of the polyplexes with CS(Dox) were prepared by mixing the aqueous solutions of the former with required volume of DMSO stock solution of the latter, and immediately vortexing for 30 seconds.

Characterization of nano-aggregates. The aggregation behaviour of the polymer-drug conjugate and its composite with pDNA polyplexes, in aqueous medium was studied. Aqueous solutions (0.02 mg/mL) in HEPES buffer of the CS, CS(CH₂COOH) and (py)CS(CH₂COOH) of different degrees of grafting were prepared from freshly sonicated stock solutions of 2 mg/mL. Similarly, the composite formulations were diluted in deionised water and used for characterization. Dynamic Light Scattering, based on photon correlation spectroscopy was used for determination of particle size and Smoluchowski model was used for determination of Zeta potential (Malvern Zetasizer Nano ZS). In a similar manner, polyplexes (prepared as mentioned above) at which complete DNA binding was observed were taken for DLS and Zeta measurements. For stability assessment, diluted (0.02 mg/mL) samples were prepared in PBS and RPMI, maintained for the respective time durations and then DLS measurement was performed. The surface morphology of the nano-aggregates was studied using Atomic Force Microscopy (AFM). Polyplexes (prepared using (py)CS(CH₂COOH) at N/P = 20), CS(Dox) and the composites were coated on Mica substrate and imaged in tapping mode by JPK instruments using NanoWizard JPK00901 software. Sizes of the polyplexes were also confirmed by taking the cross section at a particular line segment on the image.

Determination of degree of DNA binding.

(a) Agarose Gel Electrophoresis. Polyplexes (0.5 µg pDNA/20 µL) with a range of charge ratios (N/P) were prepared as described above. These were mixed with 6X DNA loading dye and electrophoresed on a 1% agarose gel at 80 V for about an hour. The gel was imaged under UV lamp (BioRad GelDoc 1000).

(b) Ethidium Bromide Fluorescence Assay. The amount of DNA condensed in polyplexes of increasing charge ratios was estimated by following the quenching of fluorescence of DNA-EtBr complex upon complexation with the polymer. Polyplexes were prepared and diluted in milli-Q water to get a final pDNA concentration equal to 7.5 µg/mL. These were loaded onto a 384-well plate in duplicate with 50 µL of polyplex solution in each well. 1.15 µL of a 0.5 mM EtBr solution was added to each well, (DNA:EtBr molar ratio of 2:1). The contents of the wells were quickly mixed and fluorescence read off using the plate reader (Varioskan Flash, ThermoScientific) by using an excitation wavelength of 511 nm.⁴ Based on emission intensity at 603 nm (I_{603}), % degree of binding was computed as

$$\% \text{ binding} = [1 - \{(I_n - I_o) / (I_m - I_o)\}] * 100 \dots\dots\dots [2]$$

where I_n is the I_{603} for a polyplex at given N/P ; I_o is the I_{603} for a well containing no DNA ; I_m is the I_{603} for DNA without the presence of polymer (representative of complete binding).

Investigation of polyplex stability.

(a) DNase resistivity. The effect of protection of the DNA against nucleases was studied as by Höggård *et al.*⁵ Three charge ratios were selected with one showing incomplete DNA binding

and two others exhibiting complete DNA binding. Polyplexes were prepared as described above with a total volume of 18 μL , containing 0.5 μg pDNA each. 2 μL of 10X reaction buffer was added followed by 0.5 units of DNase. These were incubated at 37 $^{\circ}\text{C}$ for 15 minutes and then 1 μL of 50 mM EDTA solution (inhibitor) was added followed by incubation at 65 $^{\circ}\text{C}$ for 15 minutes. The samples were cooled to room temperature, mixed with 6X DNA loading dye, loaded onto a 1 % agarose gel and run at 80 V for about 30 minutes. For each case, samples without addition of DNase were also taken as controls in adjacent lanes. The gels were imaged under UV lamp (BioRad GelDoc 1000).

(b) Heparin resistivity. The polyplexes were investigated for their stability upon exposure to increasing amounts of heparin, which is a common physiological polyanion, known to have the highest negative charge density among all known biological molecules. The destabilization effect of heparin was explored with respect to both, heparin: DNA charge ratio ($q_{\text{hep}}/q_{\text{DNA}}$) and polymer:DNA charge ratio (N/P). Degree of destabilization was measured in terms of recovery of fluorescence signal of DNA-EtBr complex. After the polyplexes were prepared, they were incubated with required amounts of heparin for two hours at room temperature.⁴ These were then loaded on to wells in a 384-well plate in duplicate with [pDNA] = 10 $\mu\text{g}/\text{mL}$ per well (0.5 μg in 50 μL). 1.15 μL of a 0.5 mM EtBr solution was added to each well, (DNA:EtBr molar ratio of 2:1). The contents of the wells were quickly mixed and fluorescence read off using the plate reader (Varioskan Flash, ThermoScientific) by using an excitation wavelength of 511 nm. Fluorescence intensity was normalized against that of DNA-EtBr complex where no polymer is present, and plotted as Relative Fluorescence Intensity (RFI). In order to confirm the observed stability towards heparin, the polyplexes, prepared as described earlier, were incubated with an

excess of heparin ($q_{\text{heparin}}/q_{\text{DNA}} = 20$) for 2 h at room temperature, after which they were loaded onto a 1 % agarose gel and run at 80 V for half an hour.

Measurement of buffering capacity of the polymer. For the assessment of pH tolerance of the polymers by way of proton sponge effect, the buffering capacity of the free polymer solutions was studied by a method similar to that of Richard *et al.*⁶ Aqueous solutions of the polymers were prepared by adding minimum amount of 0.1N HCl wherever needed for solubility. The pH of the solution was adjusted to 10 using a stock 0.1N NaOH solution. This solution was then back titrated with 0.1N HCl and pH at each step was recorded. Titration curves were plotted and buffering capacity was estimated from the slope of the curves in the region physiological pH (7.4) upto lysosomal pH (4-5).

pH dependent drug release assay. For the assessment of pH-sensitive drug release property of the polymer oxime ether linked conjugate, UV-visible spectroscopy was performed. The nano-aggregates separated from the free drug, were divided in three parts and each was resuspended in the respective buffer by vortexing. For pH 7.4 and pH 6, phosphate buffered saline was used and for pH 5, sodium acetate buffer was used. The release of Dox from the nano-aggregates was followed by recording absorbance (A) at 590 nm of the supernatant at different time intervals. The % release was calculated using the formula: $[\{ 1 - (A_t/A_o) \} \times 100]$ where t and o represent the time at which the absorbance was measured and the initial time respectively.

Critical Aggregation Concentration (CAC) determination. Fluorescence spectroscopy was performed in order to calculate CAC of the nanocomposite formulation. A stock solution of the formulation was used to prepare a 120 $\mu\text{g/mL}$ solution in PBS. The fluorescence emission spectrum was recorded with excitation at 480 nm while performing serial double dilutions. The

value of emission intensity at 590 nm obtained at each concentration was plotted against the log(concentration) values and the CAC was computed from the value at which I_{590} changed sharply.

REFERENCES

1. Park, J. H.; Cho, Y. W.; Chung, H.; Kwon, I. C.; Jeong, S. Y. Synthesis and Characterization of Sugar-bearing Chitosan Derivatives: Aqueous Solubility and Biodegradability. *Biomacromolecules* **2003**, *4*, 1087-1091.
2. Anderson, B. C.; Mallapragada, S. K. Synthesis and Characterization of Injectable, Water-soluble Copolymers of Tertiary Amine Methacrylates and Poly(ethylene glycol) Containing Methacrylates. *Biomaterials* **2002**, *23*, 4345–4352.
3. Mao, S.; Shuai, X.; Unger, F.; Simon, M.; Bi, D.; Kissel, T. The Depolymerization of Chitosan: Effects on Physicochemical and Biological Properties. *Int. J. Pharm.* **2004**, *281*, 45–54.
4. Danielsen, S.; Strand, S.; Davies, C. L.; Stokke, B. T. Glycosaminoglycan Destabilization of DNA–Chitosan Polyplexes for Gene Delivery Depends on Chitosan Chain Length and GAG Properties. *Biochim. Biophys. Acta* **2005**, *1721*, 44–54.
5. Koping-Höggård, M.; Tubulekas, I.; Guan, H.; Edwards, K.; Nilsson, M.; Varum, K.M. Chitosan as a Nonviral Gene Delivery System. Structure–Property Relationships and Characteristics Compared with Polyethylenimine In Vitro and After Lung Administration In Vivo. *Gene Ther.* **2001**, *8*, 1108–1121.
6. Richard, I.; Thibault, M.; Crescenzo, G. D.; Buschmann, M. D.; Lavertu, M. Ionization Behavior of Chitosan and Chitosan–DNA Polyplexes Indicate that Chitosan has a Similar Capability to Induce a Proton-Sponge Effect as PEI. *Biomacromolecules* **2013**, *14*, 1732–1740.